Report

Current Biology

Tooth Loss Precedes the Origin of Baleen in Whales

Highlights

- *Maiabalaena nesbittae* is 33 million year old fossil baleen whale from Oregon
- *Maiabalaena* has neither teeth, nor baleen
- Early whales lost teeth entirely before the evolutionary origin of baleen
- Despite no teeth or baleen, these whales were effective suction feeders

Authors

Carlos Mauricio Peredo, Nicholas D. Pyenson, Christopher D. Marshall, Mark D. Uhen

Correspondence

cperedo@masonlive.gmu.edu

In Brief

Peredo et al. report *Maiabalaena nesbittae*, a new genus and species of fossil whale that provides key evidence for the loss of teeth and origin of baleen. *Maiabalaena* had neither teeth nor baleen—it represents a surprising intermediate stage between modern filter-feeding whales and their toothed ancestors. Instead, *Maiabalaena* was a suction feeder.

Peredo et al., 2018, Current Biology *28*, 3992–4000
December 17, 2018 © 2018 Elsevier Ltd.
https://doi.org/10.1016/j.cub.2018.10.047

CellPress

CellPress

Current Biology
Report

Tooth Loss Precedes the Origin of Baleen in Whales

Carlos Mauricio Peredo,[1,2,6,*] Nicholas D. Pyenson,[2,3] Christopher D. Marshall,[4] and Mark D. Uhen[5]
[1]Department of Environmental Science and Policy, George Mason University, 4400 University Drive, Fairfax, VA 22030, USA
[2]Department of Paleobiology, National Museum of Natural History, PO Box 37012 MRC 121, Washington D.C. 20560, USA
[3]Departments of Mammalogy and Paleontology, Burke Museum of Natural History and Culture, 1413 NE 45th Street, Seattle, WA 98105, USA
[4]Department of Marine Biology, and Department of Wildlife and Fisheries Sciences, Texas A&M University, 200 Seawolf Parkway, Galveston, TX 77554, USA
[5]Department of Atmospheric, Oceanic, and Earth Sciences, George Mason University, 4400 University Drive, Fairfax, VA 22030, USA
[6]Lead Contact
*Correspondence: cperedo@masonlive.gmu.edu
https://doi.org/10.1016/j.cub.2018.10.047

SUMMARY

Whales use baleen, a novel integumentary structure, to filter feed; filter feeding itself evolved at least five times in tetrapod history but demonstrably only once in mammals [1]. Living baleen whales (mysticetes) are born without teeth, but paleontological and embryological evidence demonstrate that they evolved from toothed ancestors that lacked baleen entirely [2]. The mechanisms driving the origin of filter feeding in tetrapods remain obscure. Here we report *Maiabalaena nesbittae* gen. et sp. nov., a new fossil whale from early Oligocene rocks of Washington State, USA, lacking evidence of both teeth and baleen. The holotype possesses a nearly complete skull with ear bones, both mandibles, and associated postcrania. Phylogenetic analysis shows *Maiabalaena* as crownward of all toothed mysticetes, demonstrating that tooth loss preceded the evolution of baleen. The functional transition from teeth to baleen in mysticetes has remained enigmatic because baleen decays rapidly and leaves osteological correlates with unclear homology; the oldest direct evidence for fossil baleen is ~25 million years younger [3] than the oldest stem mysticetes (~36 Ma). Previous hypotheses for the origin of baleen [4, 5] are inconsistent with the morphology and phylogenetic position of *Maiabalaena.* The absence of both teeth and baleen in *Maiabalaena* is consistent with recent evidence that the evolutionary loss of teeth and origin of baleen are decoupled evolutionary transformations, each with a separate morphological and genetic basis [2, 6]. Understanding these macroevolutionary patterns in baleen whales is akin to other macroevolutionary transformations in tetrapods such as scales to feathers in birds.

RESULTS

Systematics

Cetacea; Pelagiceti; Neoceti; Mysticeti; *Maiabalaena nesbittae* gen. et sp. nov.

Etymology

Maiabalaena combines *Maia-*, meaning mother, and *-balaena*, meaning whale. Named for its phylogenetic position as basal to baleen-bearing mysticetes. The specific epithet *nesbittae* honors Dr. Elizabeth A. Nesbitt for her lifetime of contribution to paleontology of the Pacific Northwest and her mentorship and collegiality at the Burke Museum of Natural History and Culture in Seattle, Washington, USA.

Holotype

USNM 314627. Partial skeleton including a nearly complete cranium including ear bones, mandibles, and hyoid elements; vertebrae; partial left and right forelimbs; and manubrium (Figures 1–4 and S1–S4).

Locality and Age

Approximately 44°37'13.34"N, 123°56'57.71"W, Lincoln County, Oregon, USA. Approximately 180 m northwest of the type locality of *Simocetus rayi* [9] (Paleobiology Database locality number 193002). Alsea Formation, early Oligocene, earliest Rupelian, approximately 33 Ma [10, 11].

Diagnosis

Maiabalaena nesbittae is diagnosed by the following combination of character states: frontal-parietal sutures that converge posteriorly with the frontals penetrating between the parietals; apex of the occipital shield represents the dorsally highest part of the cranium; supramastoid crest extending past the posterior margin of the temporal fossa but not to the distal tip of the zygomatic process; length of the squamosal fossa is less than three-fourths the length of the temporal fossa; triangular coronoid process of the mandible that is anteroposteriorly longer than it is dorsoventrally tall; and a spear shaped distal mandibular terminus in lateral view.

(legend on next page)

DISCUSSION

We recover *Maiabalaena* as the sister taxon to *Sitsqwayk cornishorum,* another edentulous mysticete from the Pacific Northwest [12]. This unnamed clade is united by the following combination of synapomorphies: a pterygoid hamulus that is expanded into a dorsoventrally flattened plate that partially floors the pterygoid sinus fossa; an outer posterior prominence of the tympanic bulla that extends posterior to the inner posterior prominence with the two separated by a deep interprominential notch; a tympanic bulla with an inner posterior pedicle present as a thin flange; a horizontal crest on the posterior surface of the medial lobe of the tympanic bulla; a mandible with a deep groove separating the mandibular condyle from the angular process; a humeral head that is vertical in lateral; and a radius that is equal to or longer than the ulna in proximodistal length.

Our phylogenetic analysis does not include *Llanocetus* or *Mystacodon*, both of which were described only recently and have not been observed by the authors. It also does not include *Coronodon*, although it does include other toothed stem mysticetes from South Carolina of similar morphology. The most recent phylogenetic analyses [7, 8] recover these three taxa in various positions relative to other toothed mysticetes such as aetiocetids and mammalodontids, but no analysis recovers them with edentulous mysticetes.

Our phylogenetic analysis recovers the clade of *Maiabalaena* + *Sitsqwayk* as the most basal branching lineage of toothless mysticetes (Figures 2 and S4). The lack of adult mineralized teeth is interpreted from several morphological features. First, the articulation of the mandible with the cranium demonstrates that -*Maiabalaena* preserves a nearly complete right palatal margin; notably, this palatal margin shows no alveoli. Second, transverse CT scans corroborate an edentulous interpretation by showing that the palatal margin lacks alveolar bone, resembling that of edentulous mysticetes rather than toothed cetaceans (Figure 3). Third, *Maiabalaena* preserves a complete right mandible that also lacks alveoli along its dorsal border. The mandible of *Maiabalaena* resembles those of edentulous mysticetes in lacking alveolar bone and having a dorsally elevated mandibular canal in the body of the mandible [13] (Figure 4). Collectively, this morphological evidence demonstrates that *Maiabalaena* lacked both an upper and lower adult dentition.

Previous hypotheses for the origin of baleen have attempted to infer the presence of baleen in fossils from osteological correlates. In crown mysticetes, deep palatal sulci on the ventral surfaces of the maxillae accommodate structures that innervate and vascularize the tissue overlying the baleen; identical sulci are absent in stem mysticetes, although much smaller foramina in the same area have been proposed as homologs, concurrent with the presence of multicusped, adult teeth on the lateral margins [4]. However, these foramina are not present in all taxa within the relevant clades, and they differ from the sulci of baleen-bearing mysticetes in size, orientation, and overall morphology [2, 6, 14]. Moreover, similar foramina have been described in the basilosaurid *Dorudon atrox* [15] (a stem cetacean). Here we identify multiple palatal foramina on the maxilla of two other basilosaurids, *Basilotritus wardii* and *Zygorhiza kochii*, and the stem odontocete *Simocetus rayi* [9]. The presence of these foramina in basilosaurids and a stem odontocete demonstrate that the structures extend outside mysticetes altogether, further casting doubt on their use for inferring baleen.

In extant mysticetes, the superficial sulci communicate internally with the superior alveolar canal (SAC) [16]. CT imaging reveals that the single palatal foramen identified by previous authors in *Aetiocetus* [4] does communicate with the SAC. This connection is unsurprising given that the SAC supplies the gingiva and upper dentition in all toothed mammals, as well as baleen in extant mysticetes. The palatal foramina of *Maiabalaena* do not visibly communicate with the SAC; instead, they are shallow, superficial, and penetrate less than 5 mm into the rostral bone (Figure 3). Our observations may be limited by CT resolution, or it may be attributed to the loss of alveolar bone and subsequent remodeling of the palatal margin. The presence of palatal foramina in stem cetaceans and odontocetes suggests that they supply the gingiva, as suggested by previous authors [2, 6, 7, 14] and as seen in toothed mammals. Therefore, there is no evidence for using palatal foramina to exclusively infer the presence of baleen. Because all extant mysticetes possess baleen, phylogenetic bracketing [17] provides a strong basis for inferring baleen in fossil taxa within crown Mysticeti. However, there is insufficient evidence for inferring baleen in stem mysticetes based solely on the absence of teeth [2, 6, 14]; we thus interpret *Maiabalaena* as a stem mysticete lacking both teeth and baleen.

Peredo et al. [2] outlined four independent, non-exclusive hypotheses for the origin of baleen: dental filtration, medial baleen, posterior baleen, and suction feeding. The dental filtration hypothesis was recently proposed for another stem mysticete, *Coronodon havensteini* [5]. Other studies have called into question both the morphological similarity to known dental filter feeders (e.g., crabeater seals, *Lobodon*) and the biomechanical viability of dental filtration in cetaceans [2, 18]. Although the morphology observed in *Maiabalaena* does not explicitly contradict the dental filtration hypotheses, its lack of teeth more strongly supports other hypotheses instead.

The lack of evidence for both adult teeth and baleen in *Maiabalaena* is incompatible with the medial baleen [4] and posterior baleen hypotheses [19], both of which argue for an evolutionary stage during which teeth and baleen are present at the same time. Each of the latter two hypotheses have been criticized because they lack a clear functional basis for a feeding mode that uses both structures simultaneously [2, 6, 14]. Moreover, the most recent phylogenetic analyses cast doubt on these hypotheses because they imply that baleen evolved twice [14]. The age and phylogenetic position of *Maiabalaena* suggests that the loss of teeth precedes the origin of baleen and provides

Figure 1. Cranial Elements of the Holotype of *Maiabalaena nesbittae*, USNM 314627

(A–G) Dorsal (A) and ventral (B) views of the holotype skull; lateral (C) view of the right mandible; dorsal (D), lateral (E), medial (F), and ventral (G) views of left tympanic bulla.

See also Figure S1–S3 and Table S2.

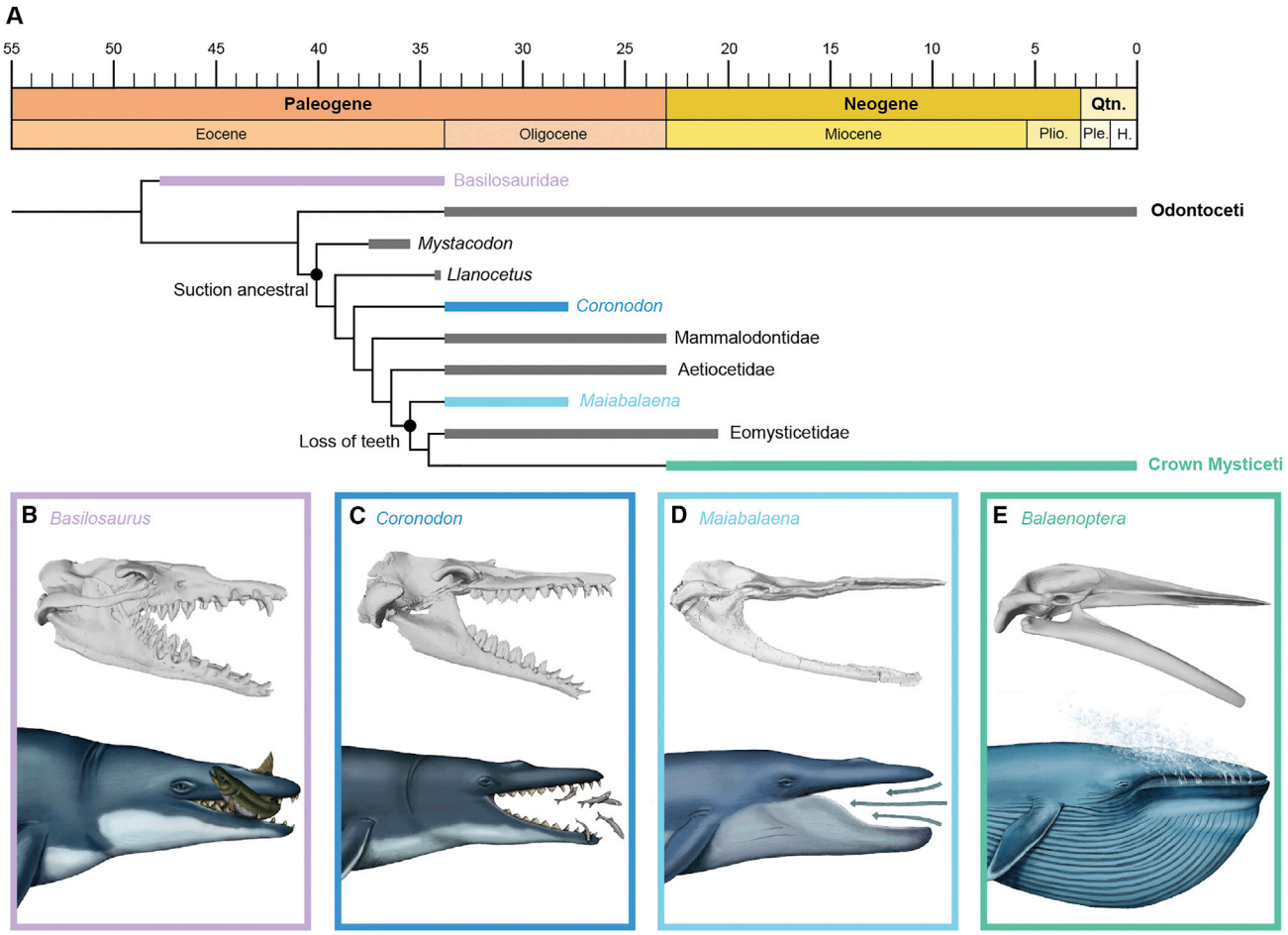

Figure 2. Phylogenetic Relationships of Stem Mysticetes Illustrating the Evolutionary Loss of Teeth and Subsequent Origin of Baleen

Figure illustrates a composite phylogeny including results from this analysis (Figure S4) and recently published analyses [5, 7, 8].

(A) Time calibrated simplified phylogeny, with collapsed clade resolution for Mammalodontidae, Aetiocetidae and Eomysticetidae, and crown Mysticeti.

(B–E) Colored bars indicate groups figured; gray bars indicate groups not figured. Panels (b–e) represent 3D models of select specimens in lateral view with artistic reconstructions of their feeding modes: (B) *Basilosaurus isis*; (C) *Coronodon havensteini*; (D) *Maiabalaena nesbittae*; and (E) *Balaenoptera musculus*. These panels illustrate the loss of a functional dentition, the intermediate phase with neither teeth nor baleen, and the subsequent origin of baleen. Illustrations are original artwork by Alex Boersma (www.alexboersma.com).

See also Figure S2.

further reason to doubt both the medial and posterior baleen hypotheses as transitional feeding modes along the lineage leading to living mysticetes.

The absence of both teeth and baleen in *Maiabalaena* is consistent with the hypothesis that tooth loss precedes the origin of baleen using suction feeding as a transitional feeding mode [2, 6, 14]. In addition to the lack of a specialized feeding structure, *Maiabalaena* preserves a large and robust hyoid apparatus (Table S1), a structure that has been correlated with suction feeding specialization in all marine mammals [20–23]. Although other mechanisms are involved in the generation of subambient pressure [22, 23], hyolingual retraction of the hyoid apparatus generates subambient pressure in suction feeding odontocetes [24] (and perhaps in an extant mysticete lineage, *Eschrichtius robustus*). Suction feeding in odontocetes is often associated with short, broad rostra and mandibles, a reduction in tooth number (or function), a limited gape, a robust and expanded basihyoid bone (in terms of surface area for muscle attachment) and teuthophagy (squid-eating [21, 24]).

However, there are important exceptions to this cetacean ecomorph theme. Several beaked whales (Ziphiidae), which are virtually edentulous, are able to generate significant subambient pressure [25] despite relatively long narrow skull and jaws. Furthermore, there are numerous accounts of individual sperm whales (*Physeter macrocephalus*) that thrive as adults despite possessing a twisted, non-functional lower jaw [26]. Soft tissue structures are known to contribute strongly to suction feeding performance in extant cetaceans [27, 28]. In spite of their long mandible, the short and wide tongue shape in sperm whales [26] is critical for producing subambient pressures at the rear of the (albeit small) oral cavity. The orofacial morphology of pygmy sperm whales (*Kogia* spp.), beluga whales (*Delphinapterus*), and other odontocetes assists in generating significant subambient pressures by occluding lateral gape and producing a

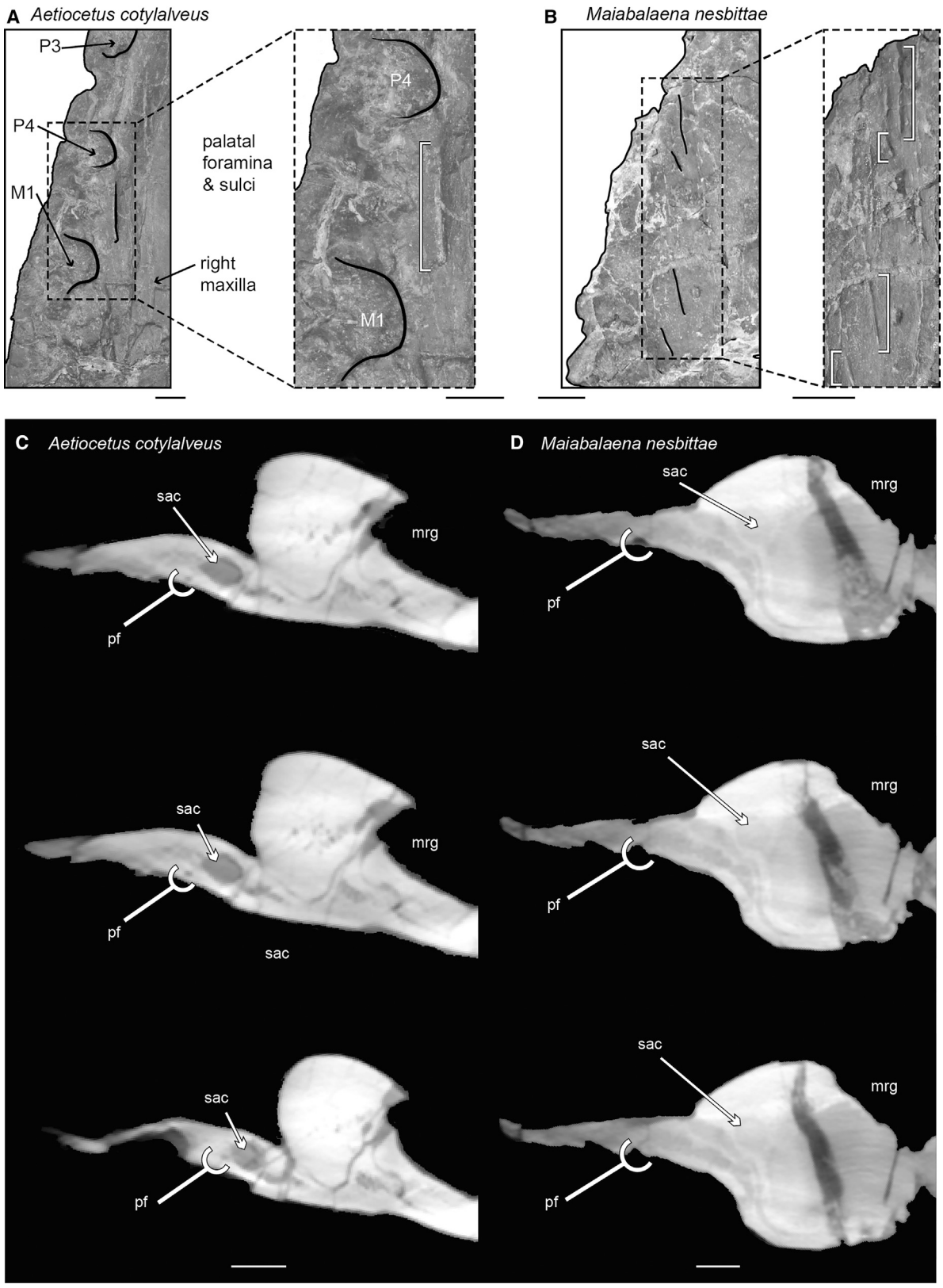

(legend on next page)

rounded pipette-like mouth opening [22, 27]. The soft connective labial eminence in many beaked whales [25, 29] functions to occlude lateral gape; similar structures in mysticetes are important in altering water flow for filter feeding [30]. Such orofacial structures are analogous to the labial cartilages of known suction-feeding elasmobranchs [31], the labial lips of suction-feeding ray-finned fishes [32], and the labial lobes of suction-feeding salamanders [33]. For beaked whales, this specific orofacial morphology favors prey capture via suction, which may be overlooked based on osteological morphology alone.

We propose that *Maiabalaena* used suction feeding as a transitional feeding mode, subsequent to tooth loss and a raptorial biting prey capture mode—but prior to the origin of baleen for filtering. Suction feeding was likely successful via a combination of a robust hyoid (in similar size and shape to other suction feeding cetaceans; see Table S1 and Data S1) and an orofacial morphology that occluded lateral gape similar to extant balaenids [30] and beaked whales [34]. Size-corrected surface area measurements of fused cetacean basihyoid and thyrohyoid bones demonstrate that the hyoid of *Maiabalaena* is substantially more robust than stem cetaceans; its surface area is also greater than those of extant mysticetes and comparable to suction feeding cetaceans (Table S1 and Data S1). Therefore, *Maiabalaena* was likely a capable suction feeder, if not a suction feeding specialist.

Notably, this ecomorph (functional edentulism and suction feeding) has evolved repeatedly in odontocetes; at least seven distinct lineages of odontocetes have evolved to feed without the aid of any specialized feeding structure (i.e., neither teeth nor baleen). This list includes both stem odontocetes (*Inermorostrum*), as well as members of several distinct crown lineages including beaked whales, sperm whales, narwhals (*Monodon*), Risso's dolphin (*Grampus*), the extinct walrus-convergent odontocete (*Odobenocetops*), and an extinct ziphiid-convergent delphinid (*Australodelphis*). This repeated convergence on functional edentulism across multiple lineages, each with distinct cranial and mandibular morphologies, suggests that tooth loss is not only viable, but advantageous for suction feeding.

At least three distinct lineages of toothed mysticetes, stemward from *Maiabalaena*, show evidence for some degree of suction feeding specialization (*Mystacodon selenensis, Mammalodon colliveri,* and an unnamed aetiocetid) [6, 8, 35]. These taxa, as well as the recently described *Llanocetus denticrenatus* [7], suggest that suction feeding evolved early in mysticete evolutionary history and perhaps represents the ancestral condition [6–8]. Fordyce and Marx [7] categorized all stem mysticetes into two broad categories: toothed forms employing suction-assisted raptorial feeding, and edentulous forms filter feeding with baleen (Figure 4 in [7]). We recover *Maiabalaena* exactly at the phylogenetic juncture between these two categories; its position and our interpretation of *Maiabalaena* as a suction-feeder lacking both teeth and baleen evince a hypothesis proposed by Marx et al. [6] and others [2, 14].

Collectively, the clade of *Maiabalaena* + *Sitsqwayk* lies crownward of all toothed mysticetes but is stemward of all other edentulous mysticetes. Data from *Maiabalaena* directly informs three basic stages in the transition from teeth to baleen: (1) toothed mysticetes including *Coronodon*, Ilanocetids, mammalodontids, and aetiocetids; (2) functionally edentulous mysticetes also lacking baleen, including *Maiabalaena* and *Sitsqwayk*, and potentially including more crownward, stem mysticetes such as eomysticetids; and (3) edentulous mysticetes filter feeding with baleen, likely including all crown mysticetes. Given that *Maiabalaena* forms a clade with *Sitsqwayk*, we tentatively infer *Sitsqwayk* as lacking both teeth and baleen, as well. Although *Sitsqwayk* lacks a rostral margin, the mandibles are well preserved and show no evidence of teeth [12].

Crownward of *Maiabalaena* + *Sitsqwayk*, edentulous mysticetes include the extinct Eomysticetidae and crown Mysticeti. Eomysticetids have traditionally been inferred as baleen-bearing based on their phylogenetic position and the presence of palatal foramina. However, palatal foramina are poor indicators of baleen [2, 7], as mentioned above (Figure 3). Recent evidence suggests that some eomysticetids may have had teeth [19, 36, 37]. In the case of *Yamatocetus*, teeth are inferred based on a scalloped palatal margin. However, this scalloping is not clearly homologous to dental alveoli, nor does the mandible preserve any evidence of a dentition, together showing no basis for interpreting teeth in *Yamatocetus*. Two other eomysticetids, *Tokarahia* and *Waharoa*, are more convincing: the former preserves an isolated tooth root assigned to the genus, and the latter preserves apparent dental alveoli at the distal tips of the mandible and rostrum. However, given that neither taxon had teeth *in situ*, these authors leave open the possibility that neither taxon had an adult dentition [19]. The presence of teeth at the distal tip of eomysticetids is not inconsistent with our hypothesis; eomysticetids clearly lacked a functional dentition, reinforcing the hypothesis that the loss of a functional dentition preceded the origin of baleen. Instead, the presence of teeth in eomysticetids strengthens the comparison of *Maiabalaena* to beaked whales [34].

The evolution of cetaceans is widely recognized as a textbook example of macroevolutionary change documented by the fossil record; few other vertebrate groups preserve such episodes of major evolutionary change. In cetacean evolution, these phases include the transition from land to sea in stem cetaceans, and evolutionary innovations associated with crown cetaceans such as echolocation in odontocetes, and filter feeding in mysticetes. In particular, filter feeding in baleen whales represents an innovation without precedent among any other extant or extinct mammalian group; explaining the origin of this complex feeding mode has been a long-standing question since Darwin [38].

The origin of filter feeding is an ecological shift that is documented by macroevolutionary transformations, akin to transition from scales to feathers in dinosaurs [39] and fins to limbs in

Figure 3. Stem Mysticete Rostra Showing Palatal Foramina

(A–D) In ventral view (anterior up, A, B) and corresponding cross sections revealed via CT scanning (dorsal side up, C, D). (A, C) *Aetiocetus cotylalveus*; (B, D) *Maiabalaena nesbittae*. Palatal foramina for *Aetiocetus* and *Maiabalaena* shown in CT cross sections represent the posteriormost palatal foramen figured in A and B, respectively. Note the internal confluence of the palatal foramen in *Aetiocetus* to the superior alveolar canal, and the absence of such confluence in *Maiabalaena.* Abbreviations—mrg: mesorostral groove; pf: palatal foramina; sac: superior alveolar canal. Scale bars represet 1 cm.

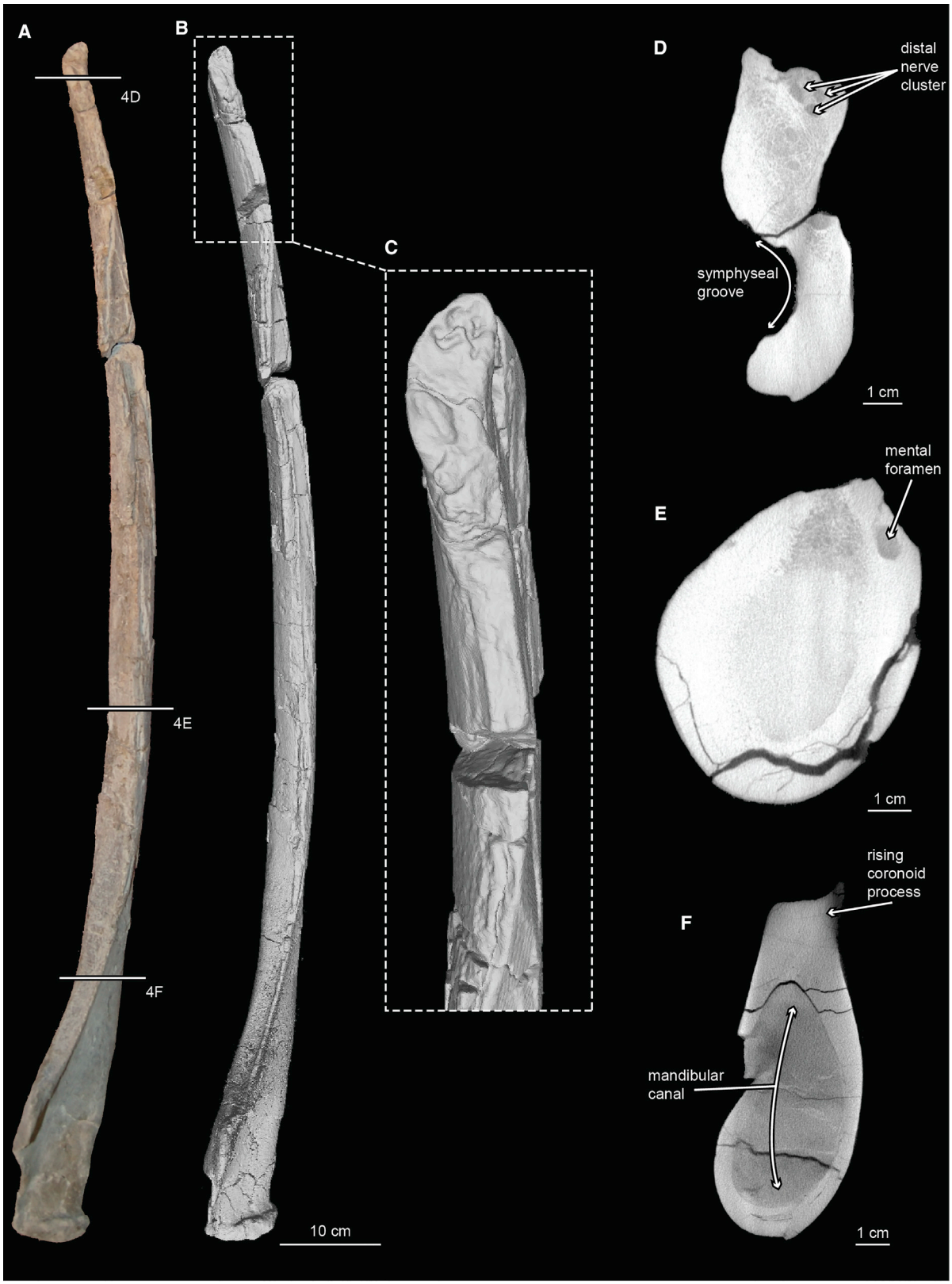

(legend on next page)

tetrapods [40]. In each case, major morphological transformations are linked to ecological transitions that fundamentally alter the natural history of the groups in question. Our study demonstrates that suction feeding in mysticetes occurred in functionally edentulous forms by the early Oligocene. This loss of teeth likely paved the way for the subsequent origin of baleen near the Oligo–Miocene boundary. The results of this study support the decoupling of tooth loss from the origin of baleen in whales; each represents a unique morphological transformation associated with a distinct change in feeding ecology.

STAR★METHODS

Detailed methods are provided in the online version of this paper and include the following:

- KEY RESOURCES TABLE
- CONTACT FOR REAGENT AND RESOURCE SHARING
- EXPERIMENTAL MODEL AND SUBJECT DETAILS
  - Institutional Abbreviations
- METHOD DETAILS
  - Digital Methods
  - Phylogenetic Analysis
  - Hyoid Surface Area Measurements
- DATA AND SOFTWARE AVAILABILITY

SUPPLEMENTAL INFORMATION

Supplemental Information including four figures, two tables, and one data file can be found with the article online at https://doi.org/10.1016/j.cub.2018.10.047.

ACKNOWLEDGMENTS

We thank C.A. Sidor, R.C. Eng, and M.S. Rivin for coordinating access to UWBM specimens and D.J. Bohaska, J.J. Ososky, M.R. McGowen and D.P. Lunde for access to USNM specimens. We thank C. Peitsch, R. Peitsch, and C. Schueler at National Technical Systems (Belcamp, Maryland), and S.B. Sholts at the SIBIR for access to resources for CT scanning. We thank E.A. Nesbitt for assistance with the stratigraphic position and age of the holotype specimen. We thank J.H. Geisler, R.W. Boessenecker, M. Brown, B.L. Beatty, and S. Boessenecker for access to the *Coronodon havensteini* 3D dataset, and the Imaging and Analysis Centre, Natural History Museum, London, for access to the *Balaenoptera musculus* 3D dataset. We thank NMNH Imaging for the photographs used throughout. Finally, we thank Alex Boersma (https://www.alexboersma.com) for the illustrations in Figure 2.

AUTHOR CONTRIBUTIONS

All authors contributed to the project planning. M.D.U. led preliminary efforts at phylogenetic analysis and comparative and systematic work. C.M.P. and N.D.P. coordinated CT scanning and modeling of digital data. C.M.P. conducted the final phylogenetic analysis and led the comparative and descriptive paleontology. C.M.P. and N.D.P. contributed to discussions of marine mammal functional feeding modes. All authors contributed to manuscript and figure preparation.

DECLARATION OF INTERESTS

The authors declare no competing interests.

Received: July 16, 2018
Revised: September 20, 2018
Accepted: October 19, 2018
Published: November 29, 2018

REFERENCES

1. Goldbogen, J.A., Cade, D.E., Calambokidis, J., Friedlaender, A.S., Potvin, J., Segre, P.S., and Werth, A.J. (2017). How baleen whales feed: the biomechanics of engulfment and filtration. Annu. Rev. Mar. Sci. *9*, 367–386.
2. Peredo, C.M., Pyenson, N.D., and Boersma, A.T. (2017). Decoupling tooth loss from the evolution of baleen in whales. Front. Mater. Sci. *4*, 1–11.
3. Esperante, R., Brand, L., Nick, K.E., Poma, O., and Urbina, M. (2008). Exceptional occurrence of fossil baleen in shallow marine sediments of the Neogene Pisco Formation, Southern Peru. Palaeogeogr. Palaeoclimatol. Palaeoecol. *257*, 344–360.
4. Deméré, T.A., McGowen, M.R., Berta, A., and Gatesy, J. (2008). Morphological and molecular evidence for a stepwise evolutionary transition from teeth to baleen in mysticete whales. Syst. Biol. *57*, 15–37.
5. Geisler, J.H., Boessenecker, R.W., Brown, M., and Beatty, B.L. (2017). The origin of filter feeding in whales. Curr. Biol. *27*, 2036–2042.e2.
6. Marx, F.G., Hocking, D.P., Park, T., Ziegler, T., Evans, A.R., and Fitzgerald, E.M.G. (2016). Suction feeding preceded filtering in baleen whale evolution. Mem. Mus. Vic. *75*, 71–82.
7. Fordyce, R.E., and Marx, F.G. (2018). Gigantism precedes filter feeding in baleen whale evolution. Curr. Biol. *28*, 1670–1676.e2.
8. Lambert, O., Martínez-Cáceres, M., Bianucci, G., Di Celma, C., Salas-Gismondi, R., Steurbaut, E., Urbina, M., and de Muizon, C. (2017). Earliest mysticete from the late Eocene of Peru sheds new light on the origin of baleen whales. Curr. Biol. *27*, 1535–1541.e2.
9. Fordyce, R.E. (2002). *Simocetus rayi* (Odontoceti: Simocetidae, New Family): A bizarre new archaic Oligocene dolphin from the eastern North Pacific. Smithsonian Contributions to Paleobiology *93*, 185–222.
10. Prothero, D.R., Bitboul, C.Z., Moore, G.W., and Niem, A.R. (2001). Magnetic stratigraphy and tectonic rotation of the Oligocene Alsea, Yaquina, and Nye Formations, Lincoln County, Oregon. In Magnetic Stratigraphy of the Pacific Coast Cenozoic, D.R. Prothero, ed. (Sante Fe Springs, CA: The Pacific Section SEPM), pp. 184–194.
11. Nesbitt, E.A. (2018). Cenozoic marine formations of Washington and Oregon: an annotated catalogue. PaleoBios *35*, 1–20.
12. Peredo, C.M., and Uhen, M.D. (2016). A new basal chaeomysticete (Mammalia: Cetacea) from the late Oligocene Pysht Formation of Washington, USA. Papers in Palaeontology *2*, 533–554.
13. Peredo, C.M., Pyenson, N.D., Uhen, M.D., and Marshall, C.D. (2017). Alveoli, teeth, and tooth loss: Understanding the homology of internal mandibular structures in mysticete cetaceans. PLoS ONE *12*, e0178243.
14. Marx, F.G., Tsai, C.-H., and Fordyce, R.E. (2015). A new early Oligocene toothed 'baleen' whale (Mysticeti: Aetiocetidae) from western North America: one of the oldest and the smallest. R. Soc. Open Sci. *2*, 1–35.
15. Uhen, M.D. (2004). Form, function, and anatomy of *Dorudon atrox* (Mammalia, Cetacea): An archaeocete from the middle to late Eocene of

Figure 4. Holotype Right Mandible of *Maiabalaena nesbittae*
(A and B) In dorsal view: (A) photograph and (B) 3D model.
(C) Enlarged view of 3D model of the distal tip of the right mandible in orthogonal view.
(D–F) Cross sections of mandible revealed via CT scanning.
White bars indicated in (A) denote the level of the cross sections.
See also Figure S2.

Egypt. The University of Michigan Museum of Paleontology Papers on Paleontology *34*, 1–222.

16. Ekdale, E.G., Deméré, T.A., and Berta, A. (2015). Vascularization of the gray whale palate (Cetacea, Mysticeti, *Eschrichtius robustus*): soft tissue evidence for an alveolar source of blood to baleen. Anat. Rec. (Hoboken) *298*, 691–702.
17. Witmer, L.M. (1995). The extant phylogenetic bracket and the importance of reconstructing soft tissues in fossils. In Functional morphology in vertebrate paleontology, J. Thomason, ed. (New York: Cambridge University Press), pp. 19–33.
18. Hocking, D.P., Marx, F.G., Fitzgerald, E.M.G., and Evans, A.R. (2017). Ancient whales did not filter feed with their teeth. Biol. Lett. *13*, 1–4.
19. Boessenecker, R.W., and Fordyce, R.E. (2015). Anatomy, feeding ecology, and ontogeny of a transitional baleen whale: a new genus and species of Eomysticetidae (Mammalia: Cetacea) from the Oligocene of New Zealand. PeerJ *3*, e1129.
20. Johnston, C., and Berta, A. (2011). Comparative anatomy and evolutionary history of suction feeding in cetaceans. Mar. Mamm. Sci. *27*, 493–513.
21. Werth, A.J. (2006). Mandibular and dental variation and the evolution of suction feeding in Odontoceti. J. Mammal. *87*, 579–588.
22. Bloodworth, B., and Marshall, C.D. (2005). Feeding kinematics of *Kogia* and *Tursiops* (Odontoceti: Cetacea): characterization of suction and ram feeding. J. Exp. Biol. *208*, 3721–3730.
23. Bloodworth, B.E., and Marshall, C.D. (2007). A functional comparison of the hyolingual complex in pygmy and dwarf sperm whales (*Kogia breviceps* and *K. sima*), and bottlenose dolphins (*Tursiops truncatus*). J. Anat. *211*, 78–91.
24. Werth, A.J. (2006). Odontocete suction feeding: Experimental analysis of water flow and head shape. J. Morphol. *267*, 1415–1428.
25. Heyning, J.E. (1996). Suction feeding in beaked whales: morphological and observational evidence. Natural History Museum of Los Angeles County Contributions in Science *464*, 1–12.
26. Werth, A.J. (2004). Functional morphology of the sperm whale (*Physeter macrocephalus*) tongue, with reference to suction feeding. Aquat. Mamm. *30*, 405–418.
27. Kane, E.A., and Marshall, C.D. (2009). Comparative feeding kinematics and performance of odontocetes: belugas, Pacific white-sided dolphins and long-finned pilot whales. J. Exp. Biol. *212*, 3939–3950.
28. Marshall, C.D., and Goldbogen, J.A. (2015). Feeding mechanisms. In Marine Mammal Physiology: Requisites for Ocean Living, M.A. Castellini, and J.-A. Mellish, eds. (CRC Press), pp. 95–118.
29. Heyning, J.E., and Mead, J.G. (1989). Contrib. Sci. *405*, 1–64.
30. Werth, A.J. (2004). Models of hydrodynamic flow in the bowhead whale filter feeding apparatus. J. Exp. Biol. *207*, 3569–3580.
31. Wilga, C.D., Motta, P.J., and Sanford, C.P. (2007). Evolution and ecology of feeding in elasmobranchs. Integr. Comp. Biol. *47*, 55–69.
32. Lauder, G.V. (1979). Feeding mechanics in primitive teleosts and in the halecomorph fish *Amia calva*. J. Zool. *187*, 543–578.
33. Deban, S.M., and Wake, D.B. (2000). Aquatic feeding in salamanders. In Feeding: form, function and evolution in tetrapod vertebrates, K. Schwenk, ed. (San Diego, CA: Academic Press), pp. 65–94.
34. Dalebout, M.L., Mead, J.G., Baker, C.S., Baker, A.N., and van Helden, A.L. (2002). A new species of beaked whale *Mesoplodon perrini* sp. n.(Cetacea: Ziphiidae) discovered through phylogenetic analyses of mitochondrial DNA sequences. Mar. Mamm. Sci. *18*, 577–608.
35. Fitzgerald, E.M.G. (2010). The morphology and systematics of *Mammalodon colliveri* (Cetacea: Mysticeti), a toothed mysticete from the Oligocene of Australia. Zool. J. Linn. Soc. *158*, 367–476.
36. Okazaki, Y. (2012). A new mysticete from the upper Oligocene Ashiya Group, Kyushu, Japan and its significance to mysticete evolution. Bulletin of the Kitakyushu Museum of Natural History and Human History Series A *10*, 129–152.
37. Boessenecker, R.W., and Fordyce, R.E. (2015). A new genus and species of eomysticetid (Cetacea: Mysticeti) and a reinterpretation of '*Mauicetus*' *lophocephalus* Marples, 1956: Transitional baleen whales from the Upper Oligocene of New Zealand. Zool. J. Linn. Soc. *175*, 607–660.
38. Darwin, C. (1872). The origin of the species by means of natural selection or the preservation of favoured races in the struggle for life, 6th Edition (London, United Kingdon: John Murray).
39. Foth, C., Tischlinger, H., and Rauhut, O.W. (2014). New specimen of *Archaeopteryx* provides insights into the evolution of pennaceous feathers. Nature *511*, 79–82.
40. Shubin, N.H., Daeschler, E.B., and Jenkins, F.A., Jr. (2006). The pectoral fin of *Tiktaalik roseae* and the origin of the tetrapod limb. Nature *440*, 764–771.
41. Peredo, C.M., and Pyenson, N.D. (2018). *Salishicetus meadi*, a new aetiocetid from the late Oligocene of Washington State and implications for feeding transitions in early mysticete evolution. R. Soc. Open Sci. *5*, 172336.
42. Goloboff, P.A., and Catalano, S.A. (2016). TNT version 1.5, including a full implementation of phylogenetic morphometrics. Cladistics *32*, 221–238.

STAR★METHODS

KEY RESOURCES TABLE

REAGENT or RESOURCE	SOURCE	IDENTIFIER
Deposited Data		
Morphological Matrix	[19, 37, 41]	N/A
Software and Algorithms		
TNT*	[42]	

CONTACT FOR REAGENT AND RESOURCE SHARING

Further information and requests for resources and reagents should be directed to and will be fulfilled by the Lead Contact, Carlos Mauricio Peredo (cperedo@masonlive.gmu.edu).

EXPERIMENTAL MODEL AND SUBJECT DETAILS

The description of *Maiabalaena nesbittae* (Data S1) is based on the holotype specimen, USNM 314627. Comparative material observed includes *Aetiocetus cotylalveus* (USNM25210), *Aetiocetus polydentatus* (cast of AMP 12), *Aetiocetus weltoni* (UCMP 122900), Chonecetus yabukii (cast of AMP 1), *Chonecetus sookensis* (NMC VP12095), *Chonecetus tomitai* (cast of AMP 2), *Coronodon havensteini* (3D model of CCNHM 108), *Fucaia buelli* (UWBM 84024), *Fucaia goedertorum* (LACM 131146), *Janjucetus hunderi* (NMV P216929), *Mammalodon colliveri* (NMV P199986), *Sitsqwayk cornishorum* (UWBM 82916), UWBM 82941, and UWBM 87135.

Institutional Abbreviations

AMP, Ashoro Museum of Paleontology; CCNHM, Mace Brown Museum of Natural History, College of Charleston, Charleston; LACM, Natural History Museum of Los Angeles County; NMC, National Museum of Canada; NMV, National Museum Victoria; UCMP, University of California Museum of Paleontology; UWBM, Burke Museum of Natural History and Culture; USNM, Smithsonian National Museum of Natural History.

METHOD DETAILS

Digital Methods

We scanned the holotype skull and mandibles of *Maiabalaena nesbittae* using Nikon Metrology's combined 225/450ckV microfocus X-ray and computed tomography (CT) walk-in vault system at National Technical Systems in Belcamp, Maryland, USA, with a slice thickness of 0.03cmm. Both the holotype skull and mandibles were scanned in storage cradles mounted vertically with the posterior side oriented down to minimize scanning width. The holotype bullae of *Maiabalaena nesbittae* were scanned using Nikon Metrology's 225ckV microfocus X-ray CT cabinet system, also at National Technical Systems, with a slice thickness of 0.03cmm. We processed DICOM files from these scans in Mimics (Materialise NV, Leuven, Belgium) to create three dimensional models of the skull, right mandible, and left bulla. High density in the basicranium hindered X-ray penetration, thus we also scanned the holotype skull using an Artec Eva structured light scanner (Artec Group, Palo Alto, California), scanning at 8 frames per second. These models are available for viewing and downloading on Zenodo at the following https://doi.org/10.5281/zenodo.1415491

Phylogenetic Analysis

We tested the phylogenetic position of *Maiabalaena nesbittae*, using the same matrix as Peredo and Pyenson [41], modified from that of Boessenecker and Fordyce [37], which already included USNM 314627 in the analysis. The final matrix includes 86 operational taxonomic units and 363 total characters. We performed a cladistic analysis using in TNT* [42] using unordered and equally weighted characters. This analysis used the 'traditional search' option including 10,000 random addition sequences, saving 10 trees per replicate. The analysis resulted in 610 most parsimonious trees with a best score of 1587 steps. The final version of this matrix is available as a separate file in the Supplemental Information. A strict consensus tree showing all operational taxonomic units is also available in the Supplemental Information (Figure S4).

This phylogenetic position of *Maiabalaena* relative to other stem mysticetes is critical to the results presented in this study. Our analysis recovers *Maiabalaena* as sister to *Sitsqwayk*, crownward of aetiocetids (and all toothed mysticetes) and basal to eomysticetids and other toothless mysticetes. *Maiabalaena* and *Sitsqwayk* are united as a clade based on seven synapomorphies presented in the main text. Here, we expand on the combination of character traits that further distinguish these taxa from other stem mysticetes, namely, eomysticetids.

The *Maiabalaena* + *Sitsqwayk* clade is sister to a clade that includes eomysticetids and all other edentulous mysticetes, including *Horopeta* and crown Mysticeti. This clade is united in this analysis by the following combination of characters: a premaxilla that is exposed in the palate only anterior to the maxilla (character 11, state 1); contact between the frontal and maxilla is loose with a developed groove (character 44, state 1); maxilla-premaxilla contact is not sutured (character 51, state 2); lacrimal is unsutured where it contacts the maxilla and frontal (character 57, state 1); a roughly straight or slightly concave dorsal edge of the orbit in dorsal aspect (character 69, state 0); optic groove positioned in the posterior third of the supraorbital process (character 85, state 1); frontal positioned at the same height as the nasals (character 86, state 1); stylomastoid fossa of the periotic developed on much of the posterior "base" of pars cochlearis (character 217, state 1); coronoid process of the mandible is a triangular process with convergent anterior and posterior margins that is higher than or equal to its length (character 265, state 2); present gingival foramina on the mandible (character 268, state 1); an absent ventral tubercle/hypophysis on the atlas and axis (character 297, state 1); a humerus with an absent lesser tuberosity (character 329, state 1).

Hyoid Surface Area Measurements

We measured the 2D surface area (in relative, scaled cm^2) of the fused basihyoid and thyrohyoids of select cetaceans in dorsal view. Hyoids were photographed in dorsal view and proportionally scaled to the same transverse width to standardize for size. 2D Surface area of the scaled hyoids was measured in ImageJ. The stylohyoids were not measured. Each specimen was measured three separate times; table S1 reports the mean values and their standard deviation, as well as each specimen as a percentage of the total size of the largest hyoid in the dataset (USNM 504345).

DATA AND SOFTWARE AVAILABILITY

The 3D models associated with this study are available for viewing and download on Zenodo at the following https://doi.org/10.5281/zenodo.1415491. The final matrix used in the phylogenetic analysis for this study is included with the supplementary materials associated with this article, available online at https://doi.org/10.1016/j.cub.2018.10.047.

Current Biology, Volume *28*

Supplemental Information

Tooth Loss Precedes the Origin of Baleen in Whales

Carlos Mauricio Peredo, Nicholas D. Pyenson, Christopher D. Marshall, and Mark D. Uhen

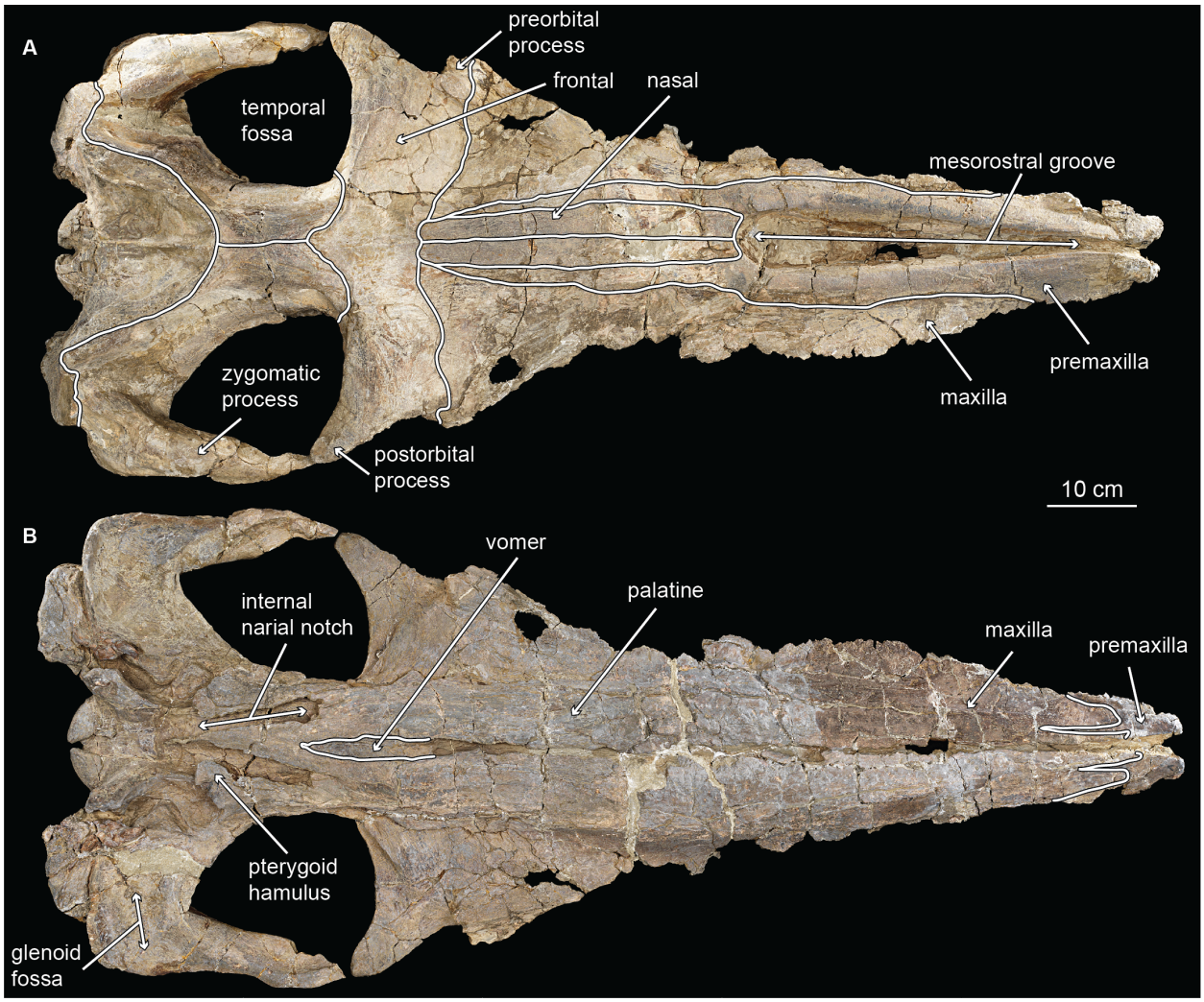

Figure S1. Holotype skull of *Maiabalaena nesbittae* (USNM 314627). Related to Figure 1. In (A) dorsal and (B) ventral views.

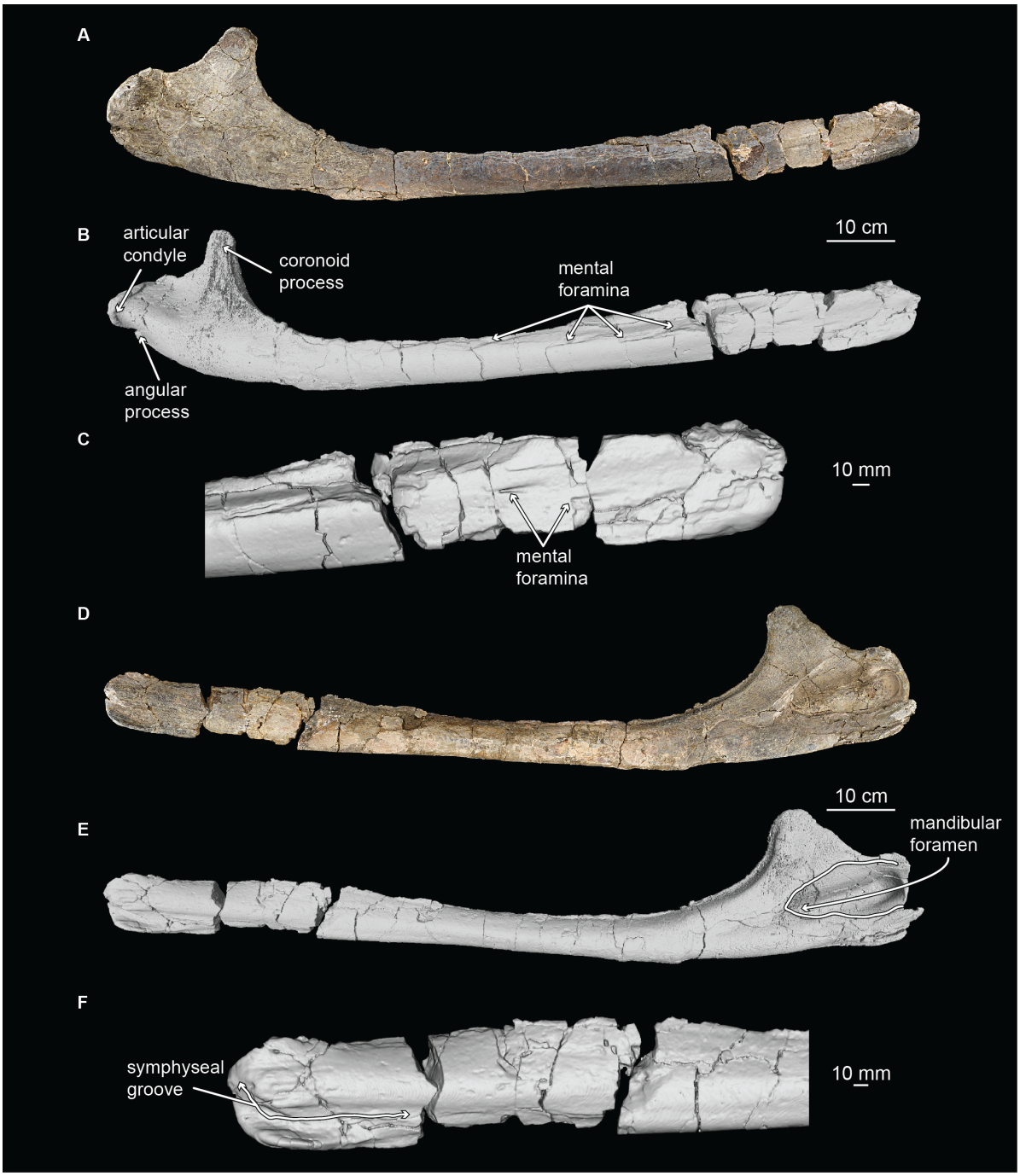

Figure S2. Holotype mandible of *Maiabalaena nesbittae* (USNM 314627). Related to Figure 1. Photographs of the lateral (A) and medial (D) views; 3D models of the complete mandible in lateral (B) and medial (E) views; and magnified view of the distal margin in lateral (C) and medial (F) views.

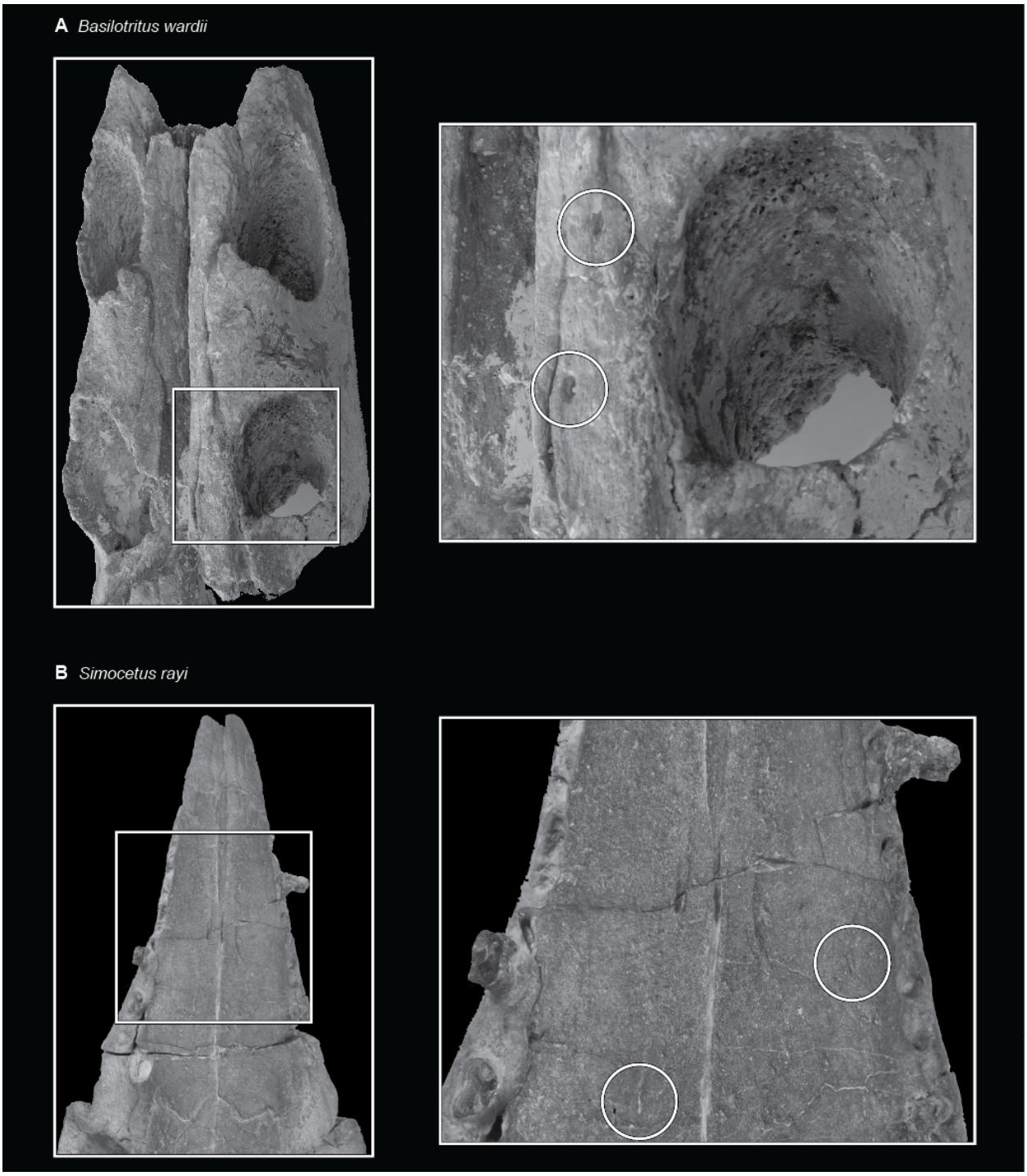

Figure S3. Palatal foramina of stem cetaceans and stem mysticetes. Related to Figure 1. (A) *Basilotritus wardii* and (B) *Simocetus rayi*.

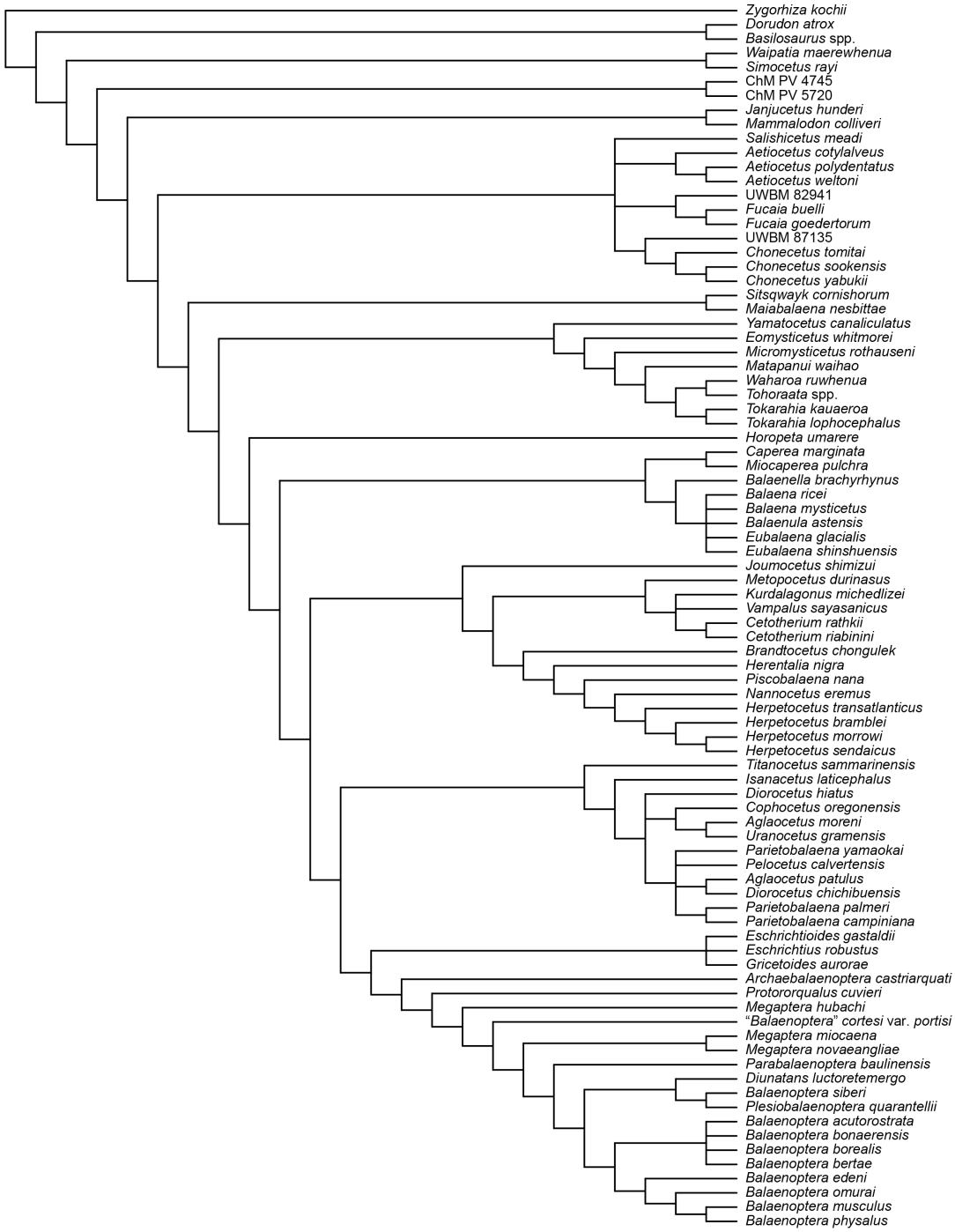

Figure S4. Strict consensus tree showing phylogenetic relationships of stem and crown mysticetes. Related to Star Methods. Phylogenetic analysis used the same matrix as Peredo and Pyenson [S1], modified from that of Boessenecker and Fordyce [S2], which already included USNM 314627 in the analysis. The analysis resulted in 610 most parsimonious trees with a best score of 1587 steps, resulting in this strict consensus tree.

Specimen	Taxon	Mean	Stan Dev	Percentage
UM 101222	*Dorudon atrox*	65.67	1.06	38.57%
USNM 314627	*Maiabalaena nesbittae**	109.44	1.76	64.28%
USNM 314627	*Maiabalaena nesbittae***	115.08	1.85	67.59%
USNM 504345	*Mesoplodon stejnegeri*	170.26	2.74	100.00%
USNM 504865	*Mesoplodon stejnegeri*	163.21	2.63	95.86%
USNM 484878	*Tasmacetus shepherdi*	140.62	0.32	82.59%
USNM 593534	*Indopacetus pacificus*	164.42	0.38	96.57%
USNM 593429	*Mesoplodon europaeus*	145.75	0.33	85.61%
USNM 572537	*Mesoplodon europaeus*	107.82	0.25	63.33%
USNM 550957	*Mesoplodon densirostris*	136.10	0.31	79.94%
USNM 504305	*Eschrichtius robustus*	93.40	1.50	54.85%
USNM 593558	*Eschrichtius robustus*	95.49	1.54	56.08%
USNM 21492	*Megaptera novaeangliae*	85.78	0.17	50.38%
USNM 49582	*Inia geoffrensis*	100.68	0.23	59.13%
USNM 395416	*Inia geoffrensis*	104.16	0.24	61.18%
USNM 172409	*Platanista gangetica*	68.26	0.16	40.09%
USNM 482707	*Pontoporia blainvillei*	105.29	0.24	61.84%
USNM 482714	*Pontoporia blainvillei*	130.11	0.30	76.42%
USNM 482713	*Pontoporia blainvillei*	137.29	0.31	80.63%
USNM 594428	*Globicephala macrorhynchus*	124.70	0.29	73.24%
USNM 550310	*Globicephala macrorhynchus*	129.94	0.30	76.32%
	*Measured as is, with part of thyrohyal missing ** Measured with thyrohyal estimated from opposite side			

Table S1: 2D surface area measurements of the hyoid apparatuses of select cetaceans in dorsal view. Related to STAR Methods. Hyoids were photographed in dorsal view and scaled to the same transverse width to standardize for size. We converted photographs into shape outlines using Adobe Illustrator and then measured 2D area in ImageJ. Each measurement was taken three times; values reported are the mean and standard deviation. Mean values are relative, scaled cm^2. See STAR methods for further details. Measurements are of the basihyoid and each thyrohyoid but exclude the stylohyoid. Percentage column is each value as a percentage of the largest surface area in the dataset (USNM 504345).

Element	Measurement	Units
Skull		**mm**
	Condylobasal length	1243.7
	Rostrum length	762.5
	Maximum width of mesorostral groove on the rostrum	64.8
	Width of rostrum at base	234.81
	Width of premaxillae at rostrum base	50.2
	Width of mesorostral groove at rostrum base	55.1
	Preorbital width	412.2
	Postorbital width	496.6
	Minimum distance between premaxillae anterior to bony nares	14.6
	Maximum width of premaxillae on cranium	24.1
	Width of bony nares	51.5
	Maximum width of nasals	33.5
	Length of medial suture of nasals	344.9
	Distance between lateral margins of premaxillae on vertex	56.9
	Maximum length of frontals on vertex	149.8
	Distance between anteromedial point of nasals and supraoccipital	582.0
	Bizygomatic width	519.3
	Length of right orbit	164.6
	Length of left orbit	167.39
	Length of right temporal fossa	179.5
	Width of occipital condyles	121.4
	Height of right occipital condyle	72.5
	Width of right occipital condyle	54.5
	Maximum distance between basioccipital crests	164.4
Periotic (right)		
	Maximum anteroposterior length	77.7
	Length of anterior process (apex anterior process to anteromedial pars cochlearis)	29.3
	Maximum width of anterior process at base	23.7
	Length of posterior process	30.3
	Width of posterior process at base, perpendicular to anteroposterior axis	17.7
	Maximum length of pars cochlearis (anteroposterior length)	33.3
	Maximum transverse width of pars cochlearis (internal edge of fenestra ovalis)	29.6

Bullae (right)		
	Total length	65.2
	Width at level of sigmoid process	32.2
	Dorsoventral depth of involucrum immediately in front of posterior pedicle	28.1
	Maximum Width	34.4
Mandible (right)		
	Straight length	1192.2
	Curvilinear length	1285.3
	Height at distal end	78.4
	Height at 50%	59.3
	Height of coronoid process	224.6
	Length of mandibular fossa	173.1
	Height of mandibular canal	49.1
Sternum		
	Length between anterior and posterior notches	96.4
	Maximum length	112.1
	Maximum width (anterior portion of later margins)	91.8
	Width at mesosternum	55.9
	Width at posterior portion	37.8
Scapula (right)		
	Anteroposterior length of glenoid fossa	102.0
	Transverse width of glenoid fossa	71.0
	Length of coracoid process	52.5
	Width of coracoid process	32.3
Humerus (right)		
	Total Length	382.0
	Transverse width of humeral head	86.5
	Anteroposterior width of humeral head	89.8
	Transverse width of greater tubercle	48.5
	Anteroposterior width of greater tubercle	67.2
	Anteroposterior width of shaft at midpoint	11.9
	Anteroposterior width at distal end	89.6
Radius (right)		
	Total length	330.0
	Width at proximal end	75.6

	Width at midpoint	77.2
	Width at distal end	68.3
Ulna (left)		
	Total length	360.2
	Length without olecranon	251.8
	Length of olecranon process	128.6
	Width at olecranon	116.2
	Width just below olecranon	76.2
	Width at midpoint	56.5
	Width at distal end	68.6

Table S2. Measurements for holotype of *Maiabalaena nesbittae* in mm. Related to Figure 1, S1.

SUPPLEMENTAL REFERENCES

S1. Peredo, C.M., and Pyenson, N.D. (2018). *Salishicetus meadi*, a new aetiocetid from the late Oligocene of Washington State and implications for feeding transitions in early mysticete evolution. Royal Society Open Science *5*, 1–22.

S2. Boessenecker, R.W., and Fordyce, R.E. (2015). A new genus and species of eomysticetid (Cetacea: Mysticeti) and a reinterpretation of '*Mauicetus*' *lophocephalus* Marples, 1956: Transitional baleen whales from the Upper Oligocene of New Zealand. Zoological Journal of the Linnean Society *175*, 607–660.

S3. Peredo, C.M., Pyenson, N.D., Uhen, M.D., and Marshall, C.D. (2017). Alveoli, teeth, and tooth loss: Understanding the homology of internal mandibular structures in mysticete cetaceans. PLOS ONE *12*, 1–26.

S4. Deméré, T.A., and Berta, A. (2008). Skull anatomy of the Oligocene toothed mysticete *Aetioceus weltoni* (Mammalia; Cetacea): implications for mysticete evolution and functional anatomy. Zoological Journal of the Linnean Society *154*, 308–352.